




Development of Transposon Mutagenesis for *Chlamydia muridarum*

Yibing Wang,^a Scott D. LaBrie,^b Steven J. Carrell,^c Robert J. Suchland,^a Zoe E. Dimond,^b Forrest Kwong,^a Daniel D. Rockey,^c P. Scott Hefty,^b  Kevin Hybiske^a

^aDivision of Allergy and Infectious Diseases, Department of Medicine, University of Washington, Seattle, Washington, USA

^bDepartment of Molecular Biosciences, University of Kansas, Lawrence, Kansas, USA

^cDepartment of Biomedical Sciences, Oregon State University, Corvallis, Oregon, USA

ABSTRACT Functional genetic analysis of *Chlamydia* has been a challenge due to the historical genetic intractability of *Chlamydia*, although recent advances in chlamydial genetic manipulation have begun to remove these barriers. Here, we report the development of the Himar C9 transposon system for *Chlamydia muridarum*, a mouse-adapted *Chlamydia* species that is widely used in *Chlamydia* infection models. We demonstrate the generation and characterization of an initial library of 33 chloramphenicol (Cam)-resistant, green fluorescent protein (GFP)-expressing *C. muridarum* transposon mutants. The majority of the mutants contained single transposon insertions spread throughout the *C. muridarum* chromosome. In all, the library contained 31 transposon insertions in coding open reading frames (ORFs) and 7 insertions in intergenic regions. Whole-genome sequencing analysis of 17 mutant clones confirmed the chromosomal locations of the insertions. Four mutants with transposon insertions in *glgB*, *pmpI*, *pmpA*, and *pmpD* were investigated further for *in vitro* and *in vivo* phenotypes, including growth, inclusion morphology, and attachment to host cells. The *glgB* mutant was shown to be incapable of complete glycogen biosynthesis and accumulation in the lumen of mutant inclusions. Of the 3 *pmp* mutants, *pmpI* was shown to have the most pronounced growth attenuation defect. This initial library demonstrates the utility and efficacy of stable, isogenic transposon mutants for *C. muridarum*. The generation of a complete library of *C. muridarum* mutants will ultimately enable comprehensive identification of the functional genetic requirements for *Chlamydia* infection *in vivo*.

IMPORTANCE Historical issues with genetic manipulation of *Chlamydia* have prevented rigorous functional genetic characterization of the ~1,000 genes in chlamydial genomes. Here, we report the development of a transposon mutagenesis system for *C. muridarum*, a mouse-adapted *Chlamydia* species that is widely used for *in vivo* investigations of chlamydial pathogenesis. This advance builds on the pioneering development of this system for *C. trachomatis*. We demonstrate the generation of an initial library of 33 mutants containing stable single or double transposon insertions. Using these mutant clones, we characterized *in vitro* phenotypes associated with genetic disruptions in glycogen biosynthesis and three polymorphic outer membrane proteins.

KEYWORDS *Chlamydia muridarum*, glycogen, *pmp*, transposon mutagenesis

Infections caused by *Chlamydia trachomatis* impose a heavy burden on public health throughout the world. *C. trachomatis* is the most common cause of bacterial sexually transmitted disease and has the highest incidence of all reportable infections (1, 2). A long-sought goal of the field is to obtain a global functional genomic understanding of the specific roles *Chlamydia* genes play in infection and pathogenesis. Historically,

Citation Wang Y, LaBrie SD, Carrell SJ, Suchland RJ, Dimond ZE, Kwong F, Rockey DD, Hefty PS, Hybiske K. 2019. Development of transposon mutagenesis for *Chlamydia muridarum*. *J Bacteriol* 201:e00366-19. <https://doi.org/10.1128/JB.00366-19>.

Editor Victor J. DiRita, Michigan State University

Copyright © 2019 American Society for Microbiology. All Rights Reserved.

Address correspondence to Kevin Hybiske, khybiske@uw.edu.

For a companion article on this topic, see <https://doi.org/10.1128/JB.00365-19>.

Received 29 May 2019

Accepted 27 August 2019

Accepted manuscript posted online 9 September 2019

Published 5 November 2019

these efforts have been hampered by a general lack of experimental systems for genetic manipulation of *Chlamydia* species. A series of advances made over the past 5 to 10 years, however, have begun to reduce these limitations (3, 4). Highlighted discoveries include the development of a stable system for genetic transformation through a shuttle vector (5), an inducible gene expression system (6), intron-based targeted gene inactivation (7), interspecies lateral gene transfer (8–10), recombination-based gene replacement (11), and forward genetics using chemically mutagenized *Chlamydia* bacteria (12–14). These new tools have greatly expanded the field's capabilities for genetic manipulation of *Chlamydia*. Functional genomic progress has also been limited by restrictions imposed by the obligate intracellular nature of *Chlamydia* and bottlenecks associated with its biphasic developmental cycle.

Chlamydial developmental growth occurs in mucosal epithelial cells within a pathogen-modified vacuole called an inclusion. From within this niche, *Chlamydia* hijacks cellular processes necessary for nutrient acquisition and maintaining a favorable replicative environment (15, 16). *Chlamydia* bacteria manipulate host cell functions with a highly streamlined genome that encodes roughly 900 proteins (17); the portion of these required for chlamydial developmental growth, or for specific *Chlamydia*-host interactions in either cell culture or *in vivo* models, is incompletely understood.

A single suicide vector system for transposon mutagenesis in *C. trachomatis* recently emerged (18). Transposon mutagenesis is an empowering, widely used strategy for generating random, single-gene insertion mutations on a genomic scale that are fixed within a chromosome and easily identified by methods such as PCR (19–21). We predicted that *Chlamydia* genes that manifest as nonessential for growth in cell culture are maintained in the genome because of selective pressures related to growth in host species. As a first step toward investigating this, we sought to establish an isogenic library of single-gene disruption mutants in the mouse-adapted species *C. muridarum*. This species is phylogenetically related to *C. trachomatis* and has been widely used in the field to model immune responses and immunopathology similar to what is found in human infections with *C. trachomatis*. *C. muridarum* infection of mice has developed into an excellent model system for the integration of contemporary genetics technologies with the examination of the roles of genes in chlamydial *in vivo* biology (22–25).

Here, we report the successful development of the Himar transposon system for *C. muridarum*. We describe the characterization of a library of isogenic mutant strains that can be used to test for virulence determinants in cell culture. We generated an initial library of 33 mutants, each containing 1 or 2 transposon insertions and many of which were genome sequenced to verify their genotypes. Across this library of mutants, a range of *in vitro* growth phenotypes were exhibited in cell culture. We describe the inability of a *glgB* transposon mutant to fully synthesize and accumulate glycogen in the inclusion lumen, and we characterize the *in vitro* defects of 3 mutant strains with transposon insertions in *pmp* genes—*pmpI*, *pmpA*, and *pmpD*.

RESULTS

Transposon mutagenesis of *C. muridarum*. We adapted the Himar transposon system for use in *C. muridarum* by modifying the nonreplicating vector used previously for introduction of transposon insertions in *C. trachomatis* L2 (18). Specifically, *bla* was replaced with *gfp-cat* (5) to produce pCMC5M (Fig. 1A). This construct allowed chloramphenicol (Cam)-based selection of *C. muridarum* mutants and screening of green fluorescent protein (GFP)-expressing plaques of *Chlamydia*-infected cells. Wild-type *C. muridarum* was transformed with pCMC5M and incubated with McCoy cells grown in multiwell plates for infection, and mutants containing transposon insertions were selected for by using Cam and monitoring of cultures for GFP-expressing bacteria (Fig. 1B). Thirty-three *C. muridarum* transposon mutants were generated from a total of 10 independent transformation experiments, and the isolated mutant strains were assigned names in numeric order from UWCM001 to UWCM033 (Fig. 1C and Table 1).

To determine the insertion sites of transposon mutants, genomic DNA (gDNA) was extracted from *C. muridarum* mutants and subjected to pyrosequencing using primers

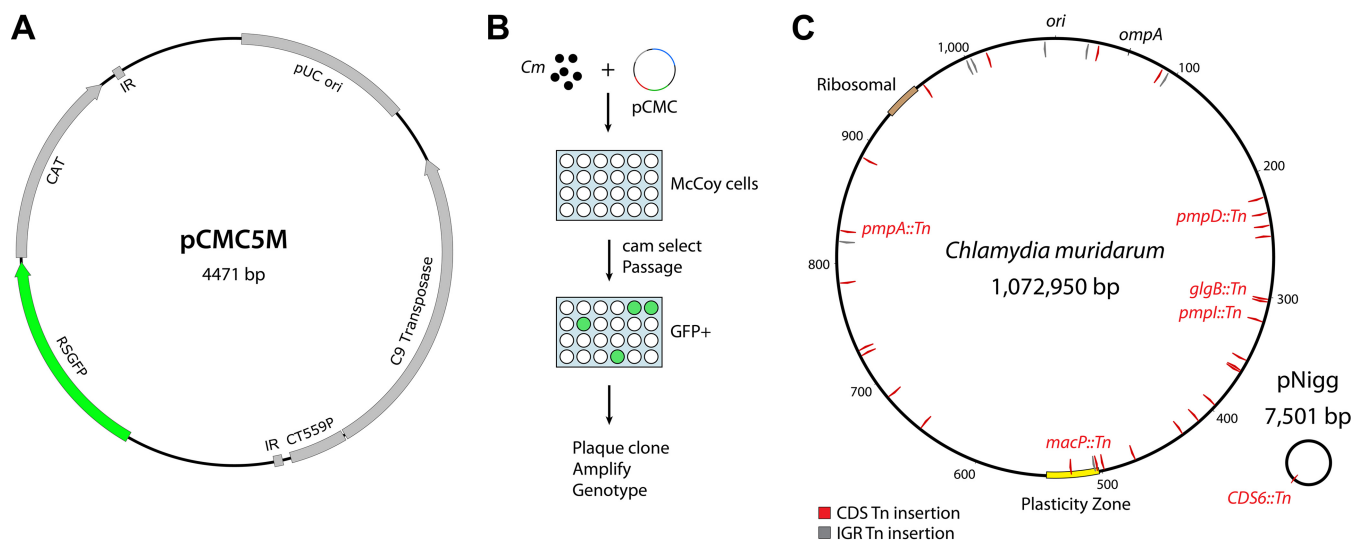


FIG 1 Generation of *C. muridarum* transposon mutants. (A) Schematic of the pCMC5M plasmid used for transformation, containing the pUC ori, Himar1 C9 transposase, and a transposon with *cat-gfp* and flanking inverted repeat (IR) sequences. (B) Overview of procedure for generating *C. muridarum* transposon mutants in McCoy cells. (C) Genome map of transposon insertions in the *C. muridarum* chromosome and plasmid pNigg. Insertions in coding sequences (CDS) are in red; insertions in intergenic regions (IGR) are in gray. Nucleotide markers on *C. muridarum* chromosome are expressed in kilobase pairs.

designed for sequences immediately inside the 5' and 3' ends of the transposed DNA. The sequencing products were analyzed by BLAST to identify candidate genomic insertion sites. For all the mutants, sequencing analysis showed that transposon insertions occurred at TA dinucleotides, with the genomic TA being replaced by the 2,003-bp transposon (Tn) as TA-transposon-TA in either orientation (Fig. 2A). To confirm the genomic locations of transposon insertions, PCR was performed on gDNA isolated from mutant strains, using primers specific to genomic sequences flanking the candidate insertion sites. Analysis showed bands that migrated 2 kb higher than wild-type (WT) *C. muridarum* parental gDNA lacking transposons (Fig. 2B).

Analysis of the transposon insertion frequency in the *C. muridarum* genome across all 33 mutants characterized during this initial study indicated that insertions occurred randomly over the genome and without notable bias (Fig. 1C). Twenty-five insertions fell within chromosomal coding regions, 7 insertions occurred within intergenic sequences, and 1 insertion was in the *C. muridarum* plasmid. Three transposon insertions were contained within the *C. muridarum* plasticity zone, a genomic region that is highly variable among species against an overall background of genomic synteny (26–28). Plasticity zone mutants were obtained for TC0431 *macP*, a MAC/perforin family protein at the 5' end of the plasticity zone; in TC0435, a phospholipase family D protein; and in TC0438, the third of three large cytotoxin/adherence factor genes that are variably present and truncated in different chlamydial strains and species (26, 29).

In 4 mutants, two separate transposon insertions occurred (Table 1 [indicated by a and b after the strain name]). Mutants with more than two insertions were not observed. An example of a double-insertion mutant was UWCM007, where genotyping of clonal plaque isolates revealed a subpopulation of mutants with a single insertion (in TC0257 *glgB*) and a second subpopulation with an identical mutation in TC0257 *glgB* and a second transposon insertion in TC0431 *macP* (Fig. 2). These plaque-cloned strains were subsequently reclassified as UWCM007 (insertions in both *macP* and *glgB*) and UWCM027 (a single insertion in *glgB*). In a lone instance (mutant clone UWCM022), transposition was associated with the deletion of approximately 2 kb of genomic DNA adjacent to the insertion, between chromosomal coordinates 361528 and 363601 (Fig. 2C). The deleted genes included TC0303 to TC0306, and the transposed DNA remained intact in this event.

Whole-genome sequence analysis. Whole-genome sequencing was performed on 17 transposon mutants. Genome sequence analysis revealed that the transposon

TABLE 1 *Chlamydia muridarum* transposon mutants

Strain ^a	Insert position (TA location) ^b	Locus	Gene	Protein	% predicted translated
UWCM001	242824>25	TC0206		Hypothetical protein	86
UWCM002	785559<60	TC0657	<i>pgi</i>	Glucose-6-phosphate isomerase	30
UWCM003	472705>06	TC0411		Inc (predicted)	99
UWCM004a	35408>09	TC0031	<i>gyrA2</i>	DNA topoisomerase IV subunit A	67
UWCM004b	730561>62	TC0610	<i>uvrA</i>	Excinuclease ABC subunit A	11
UWCM005	1018583	TC0878		Hypothetical protein	11
UWCM006	818430<31	IGR			
UWCM007a	301598>99	TC0257	<i>glgB</i>	14-Alpha-glucan-branching protein	86
UWCM007b	498439>40	TC0431	<i>macP</i>	MAC/perforin family protein	8
UWCM008	303619>20	TC0259		Hypothetical protein	90
UWCM009	220664>65	TC0189		Hypothetical protein	77
UWCM010	363126>27	TC0305		Hypothetical protein	80
UWCM011	687198<99	TC0575	<i>pknD</i>	Serine/threonine protein kinase	7
UWCM012	827362<63	TC0693	<i>pmpA</i>	Outer membrane protein PmpA	77
UWCM013	413657<58	TC0350	<i>folD</i>	Bifunctional 5,10-methylene-tetrahydrofolate dehydrogenase/cyclohydrolase	25
UWCM014a	232911>12	TC0197	<i>pmpD</i>	Outer membrane protein PmpD	67
UWCM014b	395719<20	TC0333	<i>gnd</i>	6-Phosphogluconate dehydrogenase	98
UWCM015	503579<80	TC0435		Phospholipase	66
UWCM016	505694>95	IGR			
UWCM017	887618<19	TC0473		Acetyltransferase	66
UWCM018	1065355<56	IGR			
UWCM019	319531<32	TC0267	<i>pmpI</i>	Outer membrane protein PmpI	70
UWCM020	94501>02	IGR			
UWCM021	26638<39	IGR			
UWCM022	361528<	TC0303		Hypothetical protein	0
	363601 ^c	TC0306		Hypothetical protein	70 ^d
UWCM023a	524741>42	TC0438		Cytotoxin/adherence factor	86
UWCM023b	1001585<86	IGR			
UWCM024	429854<55	TC0368	<i>ribF</i>	Bifunctional riboflavin kinase/FMN adenylyltransferase	2
UWCM024		TC0369	<i>truB</i>	tRNA pseudouridine synthase B	98
UWCM025	726016>17	TC0606		Exodeoxyribonuclease 7 small subunit	32
UWCM026	251258<59	TC0212	<i>rmuC</i>	DNA recombination protein RmuC homolog	60
UWCM027	301598>99	TC0257	<i>glgB</i>	1,4-Alpha-glucan branching protein	86
UWCM028	1006942<42	IGR			
UWCM029	4770>71 ^e	CDS6		pNigg CDS6	64
UWCM030	641212<13	TC0530		Protein phosphatase	72
UWCM031	358972<73	TC0302	<i>recD</i>	ATPase AAA	86
UWCM032	959708<09	TC0828	<i>mip</i>	Peptidyl-prolyl <i>cis-trans</i> isomerase	15
UWCM033	87859<60	TC0075		Hypothetical protein	22

^aa and b indicate two separate transposon insertions.

^bGenome location on *C. muridarum* chromosome (NC_002620); > and < indicate the orientation of the *gfp-cat* transposon in the genome.

^cInsert occurred with a 2,072-bp deletion beginning at 361529; genes TC0304 and TC0305 were deleted.

^dTruncation due to transposon insertion occurred at the 3' end of TC0306.

^eGenome location on *C. muridarum* plasmid pMoPn (NC_002182).

insertions were intact in these mutants and confirmed that the insertions were at the TA locations indicated by PCR and Sanger sequencing. Whole-genome sequencing of the *C. muridarum* parent strain used to create the transposon library showed the presence of 41 single nucleotide variants (SNVs) from the reference strain NC_02620 (see Table S1 in the supplemental material). The *C. muridarum* parent contained noted variants in the poly(G) tracts of two phospholipase family proteins, TC0436 and TC0447. No additional SNVs or other mutations, for example, compensatory mutations from propagation of transposon mutants, were identified in the transposon mutants.

Stability of transposon insertions in *C. muridarum*. We investigated whether transposon insertions were stable during long-term propagation of mutant strains in the absence of selection. Two plaque-purified transposon mutants, *pmpA*::Tn and *glgB*::Tn mutants, were passaged for 10 generations either with or without 0.5 μ g/ml Cam. Following serial passage, gDNA was extracted from the mutant strains, and the presence of each transposon insert was analyzed by PCR using primers flanking the insertion sites. PCR analysis showed that high-molecular-weight products—indicating

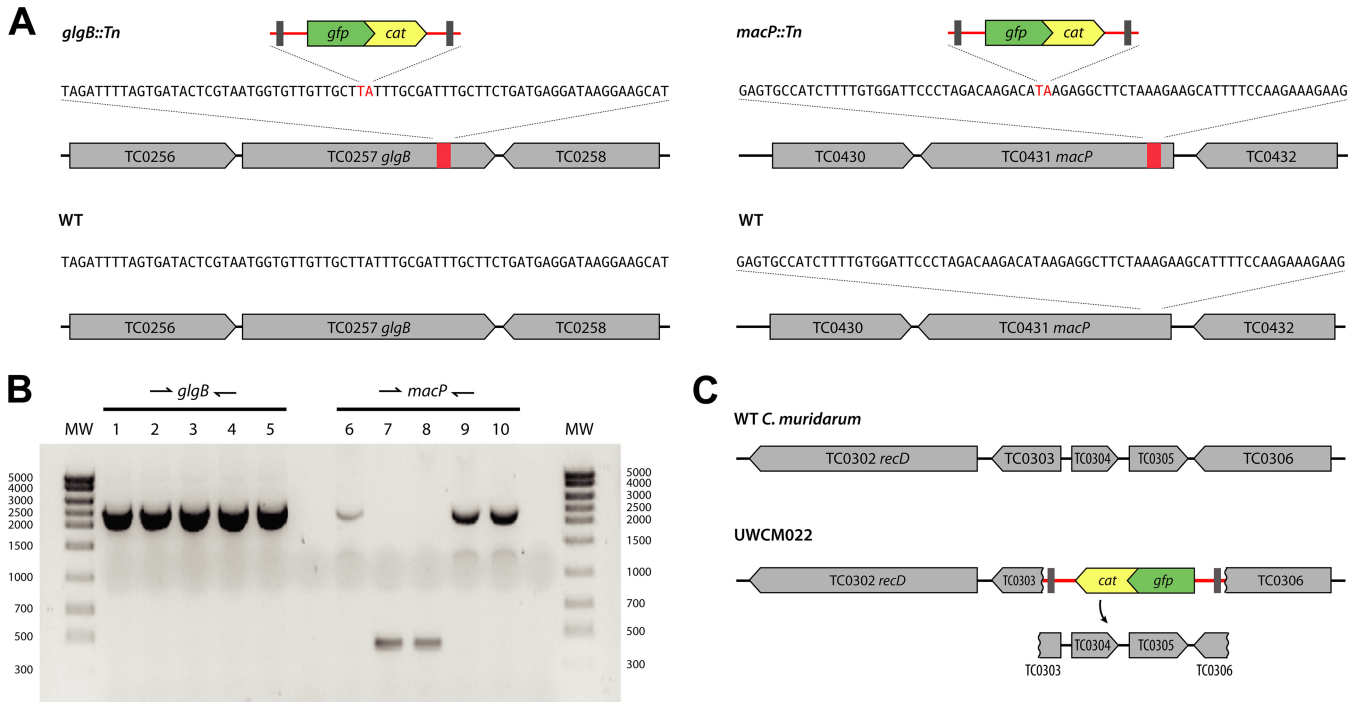


FIG 2 Transposon insertions in *glgB* and *macP*. (A) Chromosomal sequences of insertion sites. (B) PCR analysis of UWCM007 using primers against flanking sequences in genomic DNA. Lanes: 1, UWCM007 (*glgB::Tn* and *macP::Tn*); 2, plaque-cloned UWCM007 (*glgB::Tn*); 3, plaque-cloned UWCM027 (*glgB::Tn*); 4, plaque-cloned UWCM007 (*glgB::Tn* and *macP::Tn*); 5, 2× plaque-cloned UWCM007 (*glgB::Tn* and *macP::Tn*); 6, UWCM007 (*glgB::Tn* and *macP::Tn*); 7, plaque-cloned UWCM007 (*glgB::Tn*); 8, plaque-cloned UWCM027 (*glgB::Tn*); 9, plaque-cloned UWCM007 (*glgB::Tn* and *macP::Tn*); 10, 2× plaque-cloned UWCM007 (*glgB::Tn* and *macP::Tn*). (C) Schematic showing the deletion of sequences between TC0303 and TC0306 that occurred with the insertion of an intact transposon (red) in mutant clone UWCM022.

the presence of transposon insertions—were present in the strains regardless of Cam selection (Fig. 3). Furthermore, low-molecular-weight bands were not present, indicating no detectable loss of fragments of the transposed DNA. Thus, the transposon insertions were stable for at least 10 passages, consistent with previous measurements (18).

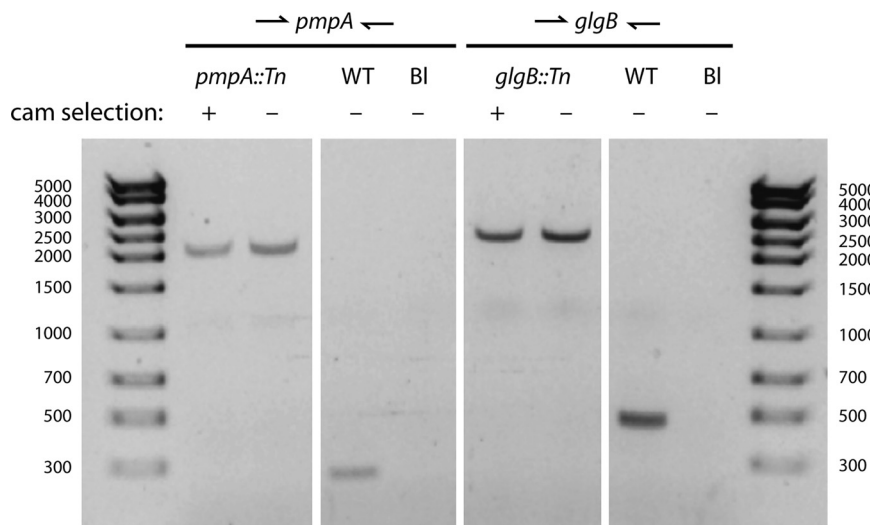


FIG 3 Stability of transposon inserts. Two plaque-purified transposon mutants, UWCM012 (*pmpA::Tn*) and UWCM027 (*glgB::Tn*), were grown continuously for 10 generations in the presence (+) or absence (–) of 0.5 μg/ml chloramphenicol (cam). Genomic DNA from the passaged strains was extracted and subjected to PCR analysis using primers designed against genomic sequences flanking the transposon inserts. The ~2-kb bands denote the sizes of transposon inserts.

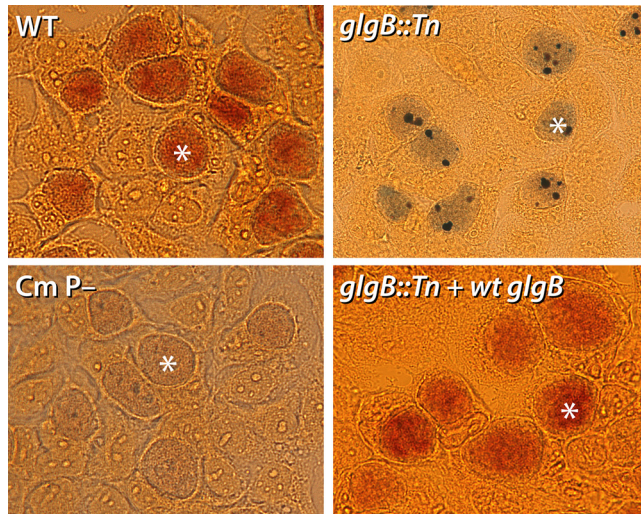


FIG 4 Deficient glycogen accumulation in *glgB::Tn* inclusions. McCoy cells were infected with WT *C. muridarum*, a *glgB::Tn* mutant, a plasmid-free strain of *C. muridarum* (Cm P⁻), or a complemented *glgB::Tn* strain expressing WT *glgB*. Iodine staining of the infected cells at 26 hpi showed WT glycogen accumulation in WT and complemented inclusions (dark orange), no glycogen in Cm P⁻ inclusions, and amylose accumulation in *glgB::Tn* inclusions (purple with dark deposits). Representative inclusions in each image are marked with asterisks.

Requirement for *glgB* in inclusion glycogen biosynthesis. The accumulation of glycogen within inclusions is a hallmark feature of some *Chlamydia* species and strains, and the trait has been linked to plasmid-regulated expression of glycogen metabolism enzymes and acquisition of UDP-glucose from the host cell (5, 13, 30, 31). To determine the role of GlgB in glycogen production inside *C. muridarum* inclusions, we compared the abilities of a *glgB::Tn* mutant clone (UWCM027) and the WT parent to synthesize and accumulate glycogen in inclusions. GlgB is a predicted 1,4- α -glucan branching protein and was expected to play a critical role in glycogen biosynthesis inside inclusions (13). McCoy cells were infected with the *glgB::Tn* mutant, WT *C. muridarum*, or a plasmid-free *C. muridarum* strain; stained with iodine at 26 h postinfection (hpi) to label glycogen; and analyzed by bright-field microscopy. Inclusions derived from the *glgB::Tn* mutant contained dark purple-black deposits representative of amylose accumulation (Fig. 4), a feature that was visually distinct from those of both the WT (accumulated glycogen) and plasmid-lacking (no-glycogen) strains (30, 32). To confirm that this phenotype was due to transposon-mediated disruption of *glgB*, we generated a complemented strain transformed with a plasmid containing WT *glgB* and *mCherry*. Iodine staining of inclusions infected with the WT-*glgB*-complemented strain (*glgB::Tn* plus WT *glgB*) demonstrated a restoration of glycogen accumulation to WT levels (Fig. 4).

In vitro phenotypes of *C. muridarum* *pmp* mutants. Three transposon insertions in the library fell within polymorphic membrane protein (*pmp*) genes (Fig. 5A), encoding a protein family with potential functions in *Chlamydia* adherence and pathogenesis (33–36). Isogenic transposon mutants therefore presented a unique opportunity to test the importance of individual Pmp proteins—PmpI, PmpA, and PmpD—for *in vitro* growth phenotypes in *C. muridarum*. The *pmpD::Tn* transposon mutant contained a second transposon insertion in *gnd*, encoding 6-phosphogluconate dehydrogenase (Table 1). In all three *pmp* mutants, transposon insertion sites lay upstream of the autotransporter domains (Fig. 5B), and therefore, the truncated proteins were predicted to be functionally disrupted. We performed growth curve analysis by infecting McCoy cells with each of the mutant strains or a control strain with an intergenic transposon insertion (IGR::Tn [IGR, intergenic region]; UWCM016), at low multiplicities of infection (MOI) and measured the amount of infectious progeny production for each strain on a

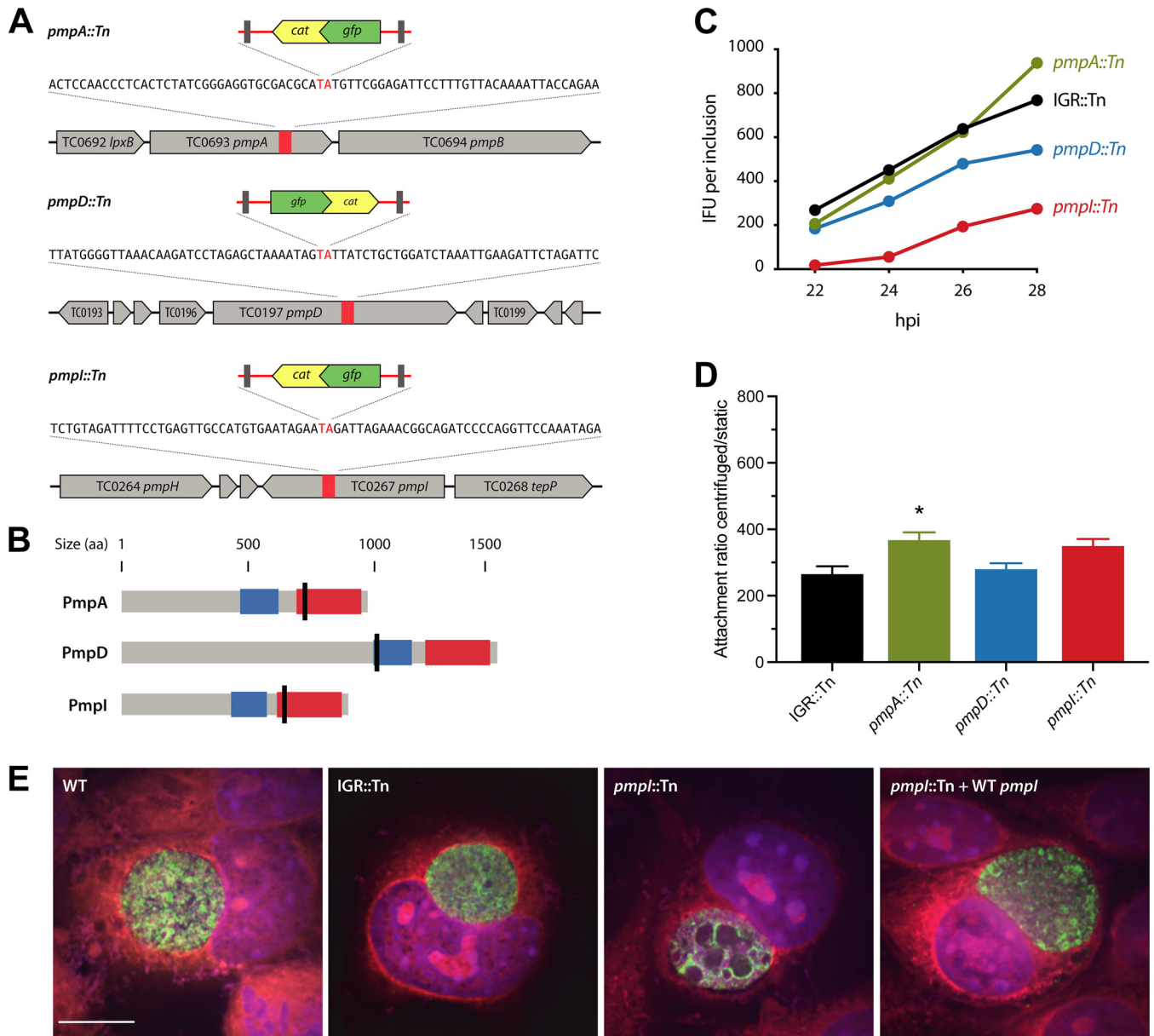


FIG 5 *In vitro* phenotypes of *C. muridarum* *pmp* mutants. (A) Chromosomal locations of transposon insertions in *pmp* genes. The orientations of inserts are indicated by the gene directionality. (B) Predicted protein topologies of Pmp proteins. Transposon insertion sites are marked with black lines; blue, Pmp middle domain; red, autotransporter domain. (C) Inclusion burst sizes of *pmpI::Tn*, *pmpA::Tn*, and *pmpD::Tn* strains versus an IGR::Tn control strain. McCoy cells infected with the indicated strains were harvested at the times postinfection indicated, and the amount of infectious progeny in each sample was determined by infecting fresh McCoy cells, followed by IFU assays. (D) Attachment of the indicated strains to McCoy cells was determined by inoculating the cells under centrifugation-aided and static conditions. The ratios of centrifugation to static conditions were computed. The data represent means, and the error bars indicate standard deviations. Statistical comparisons between transposon mutants and the IGR::Tn control were analyzed using one-way ANOVA with Dunnett's test for multiple comparisons. *, $P < 0.05$. (E) Confocal immunofluorescence analysis of inclusions containing WT *C. muridarum*, the IGR::Tn or *pmpI::Tn* mutant, and the complemented *pmpI::Tn*-plus-WT *pmpI* strain analyzed at 24 hpi. Green, anti-LPS; blue, DAPI; red, Evans blue. Scale bar, 10 μ m.

per-inclusion basis over 22 to 28 hpi. UWCM016 was selected as a control over other IGR::Tn mutants because the transposon in the mutant was over 250 and 600 nucleotides away from the nearest, diverging genes. Compared to the IGR::Tn control strain, the *pmpI::Tn* mutant exhibited significant attenuation across all the times examined—64% fewer infectious progeny than the IGR::Tn strain at 28 hpi (Fig. 5C). The *pmpD::Tn* mutant was also partially attenuated for growth, with 30% reduced progeny formation at 28 hpi compared to the IGR::Tn strain. The *pmpA::Tn* mutant exhibited no growth attenuation; however, it reproducibly produced greater amounts of infectious elemen-

tary bodies (EB) at 28 hpi only, 122% of the EB produced by the IGR::Tn strain (Fig. 5C). We tested whether the presence of the transposon had any deleterious effect on chlamydial growth by comparing propagation ratios between the IGR::Tn control and WT *C. muridarum*, and we measured similar levels of inclusion-forming unit (IFU) production for both control strains (745 ± 69 for the WT and 739 ± 37 for the IGR::Tn strain) (data not shown). The enhanced progeny formation phenotype of the *pmpA*::Tn strain correlated with an abundance of floating *Chlamydia*-containing objects above the *pmpA*::Tn mutant-infected cell monolayer (see Fig. S1 in the supplemental material). These objects resembled chlamydial extrusions (37, 38); however, we do not have an explanation or hypothesis for why this particular mutant would produce either more extrusions or more stable ones. The observations were nonetheless reproducible, and it was not pursued further because of its minor contribution to *pmpA*::Tn phenotypes.

We next characterized *Chlamydia* cell and inclusion morphologies within host cells infected with *pmp* transposon mutants. L929 mouse fibroblasts were infected with WT *C. muridarum*, IGR::Tn, *pmpI*::Tn, and *pmpI*::Tn-plus-WT *pmpI* strains and analyzed by immunofluorescence microscopy at 24 hpi. Antilipooligosaccharide (anti-LOS) immunofluorescence revealed that every *pmpI*::Tn inclusion contained enlarged, abnormal-size bodies within the chlamydial inclusion (see Fig. S2 in the supplemental material). *pmpI*::Tn plus WT *pmpI* restored the phenotype of *pmpI*::Tn to wild-type phenotypic conditions (Fig. 5E). Inclusions derived from the *pmpA*::Tn mutant appeared WT in terms of general morphology, as did *pmpA*::Tn-plus-WT *pmpA* mutant-derived inclusions (see Fig. S3 in the supplemental material). Inclusions containing *pmpD*::Tn mutants mostly exhibited bacteria and inclusion morphologies and distributions like those containing WT *C. muridarum*. Approximately 30% of *pmpD*::Tn inclusions contained abnormally dispersed bacteria (see Fig. S3).

Pmp proteins have been reported to play roles in *Chlamydia* attachment to host cells, including *C. pneumoniae* (33, 36, 39) and *C. trachomatis* (10). We investigated whether PmpA, PmpD, or PmpI individually contributed to *C. muridarum* binding to McCoy cells by measuring attachment under centrifugation-aided versus static conditions. Cells were infected with each *pmp*::Tn mutant or an IGR::Tn control using a low MOI to ensure that the resulting inclusions were derived from individual bacteria. Parallel infections were performed with centrifugation or in static culture, and at 20 to 22 hpi, the cells were lysed, the numbers of infectious EB were determined by infecting fresh McCoy cells, and the numbers of IFU per original inclusion were back calculated. The overall attachment efficiencies for all *C. muridarum* strains were low, and determination of the ratios of inclusion burst sizes under centrifugation and static conditions showed minimal differences attributable to each of the *pmp* mutants (Fig. 5D). There appeared to be a slight trend toward reduced attachment of *pmpI*::Tn and *pmpA*::Tn mutants under static conditions (Fig. 5D).

Complementation of transposon mutants restored *in vitro* growth phenotypes.

To validate the genotypes of *glgB* and *pmp* genes, we generated complemented strains containing plasmid-borne *mCherry* and WT *glgB*, WT *pmpI*, or WT *pmpA*. Complemented genes were placed under the control of their endogenous promoters, and *mCherry* was constitutively expressed. The *pmpD*::Tn mutant was not included for complementation analysis due to the large size of the *pmpD* gene and weak phenotypes associated with the mutant. For each complemented strain, the capacity for complete inclusion growth was determined by measuring IFU on a per-inclusion basis, using serial infections with low-MOI inocula. Compared to cells infected with the IGR::Tn strain, *glgB*::Tn mutant-infected cells produced 23% fewer IFU (Fig. 6). The small growth defect due to transposon disruption of *glgB*, while not statistically significant, was overcome by complementation with plasmid-expressed WT *glgB* (Fig. 6). These data for *glgB* are consistent with previous findings for *glgB* mutants in *C. trachomatis* (13). Cells infected with *pmpI*- and *pmpA*-complemented strains also exhibited restored growth phenotypes (Fig. 6).

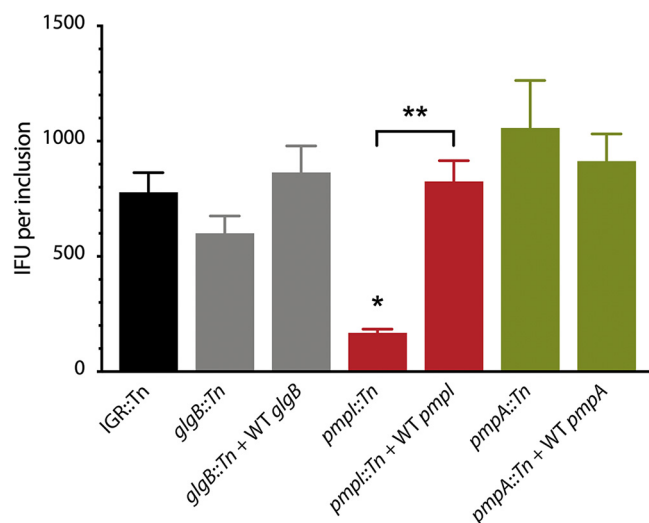


FIG 6 *In vitro* growth phenotypes of transposon mutants and complemented strains. The growth of mutants and complemented strains was assessed by the IFU propagation ratio. McCoy cells were infected with each strain in 24-well plates. At 20 to 22 hpi, images were taken for inclusion counting by fluorescence microscopy. At 26 hpi, the cells were lysed and the bacteria were inoculated onto fresh McCoy cells for IFU determination. The data are expressed as means, and the error bars indicate standard deviations. Statistical comparisons between the transposon mutants, complemented strains, and IGR::Tn control were analyzed using one-way ANOVA with Dunnett's test for multiple comparisons. *, $P < 0.05$; **, $P < 0.01$.

DISCUSSION

An increasing number of genetic tools have emerged for genetic manipulation of *Chlamydia* (4, 40). The recent development of a transposon mutagenesis system for *C. trachomatis* L2/434 by Hefty and colleagues adds a powerful new technique to this growing repertoire of chlamydial genetic techniques (18). This study expands on the transposon technological platform by adapting it for use in the rodent species *C. muridarum*. The development of a transposon mutant library in *C. muridarum* provides two important advantages. First, it enables functional genetic analysis of homologous chlamydial gene products across two *Chlamydia* species. Second, it allows the screening of chlamydial genes for critical *in vivo* functions in their matched host species. Functional genetic studies in cell culture are likely not the best model for *Chlamydia*, based on evidence that particular loci rapidly accumulate disruptive mutations during adaptation of *C. trachomatis* to cell culture and mice (41, 42). Thus, we expect that the growing availability of isogenic transposon mutants in *C. muridarum* will be a valuable resource for investigators in the field.

The distribution and frequency of transposon insertions in this initial library suggest that transposon insertions occurred without chromosomal bias. Consequently, the eventual generation of a saturation library in genes and operons that can tolerate disruption is feasible. As for *C. trachomatis*, the critical bottleneck limiting the generation of transposon mutants is getting DNA into the bacteria. This limitation continues to be a major factor for most genetic-engineering applications in *Chlamydia* (4, 5). Based on previous genome-wide chemical mutagenesis findings, where 75 unique nonsense mutants were obtained (14), one can speculate on how many transposon mutants are necessary to achieve saturation levels of mutagenesis. We have run statistical modeling and determined that a library of 1,000 mutants would cover 599 of ~890 *Chlamydia* open reading frames (ORFs); 2,000 mutants would cover 784 ORFs with 1,216 duplicate hits. This library size likely would approach saturation levels of mutagenesis. Our *C. muridarum* library contains transposon insertions in coding and intergenic regions, and while the majority of inserts were in the chromosome, a mutant was obtained in the *C. muridarum* plasmid. Curiously, several mutant clones harboring two transposon insertions were obtained. This is in contrast to *C. trachomatis*, where

only mutants with single insertions were derived across nearly 100 mutant strains (18). The simplest explanation for the occurrence of double insertions is that it was an outcome of two or more plasmid copies entering a bacterium, allowing the mobilization of two transposons into the chromosome. Supporting evidence for this comes from analysis of mutant UWCM007, which contained transposon insertions in TC0257 *glgB* and TC0431 *macP*. Subsequent whole-genome sequencing analysis of plaque clones from this parent mutant strain showed the presence of two subpopulations—one containing an insert in TC0257 *glgB* and another containing inserts in the same location in TC0257 *glgB* and additionally in TC0431 *macP*. The likeliest explanation for the generation of these mutant clones is that a first insertion occurred in TC0257 *glgB* and, after some chlamydial replication, a second insertion occurred from residual plasmid in TC0431 *macP* in a single daughter cell. An alternative explanation, given the low efficiency of DNA delivery into *Chlamydia* and the observation that double insertions have not yet been detected in *C. trachomatis* (18), is different mechanisms of drug selection—chloramphenicol in *C. muridarum* and penicillin in *C. trachomatis*. The bacteriostatic effect of chloramphenicol could enable the relatively rare double molecule uptake and transposon insertion. Additional possibilities include the contribution of marker removal by recombination with wild-type genomes, or possibly low-level pCMC5M plasmid replication, to the generation of double transposon insertions.

Among the diversity of transposon mutants generated in this study, 4 particular insertions were selected for follow-up investigation based on the predicted biological functions of the disrupted genes in *Chlamydia* infections. The importance of the chlamydial enzymes GlgA and GlgX for glycogen biosynthesis and accumulation in the inclusion lumen has been characterized for *C. trachomatis* (5, 30, 31, 43). Furthermore, a GlgB *C. trachomatis* mutant strain derived from chemical mutagenesis was shown to be defective in converting unbranched to branched glycogen in the inclusion lumen (13). Our data using the *glgB*::Tn isogenic mutant confirmed that the glycogen-debranching enzyme GlgB plays a similarly important role for glycogen biosynthesis in *C. muridarum* inclusions and additionally demonstrates that GlgB-deficient *C. muridarum* bacteria accumulate the glycogen intermediate amylose in their inclusion lumens. We expect that the isolation of transposon insertions in additional genes predicted to play roles in chlamydial glycogen biosynthesis, through expansion of the transposon mutant library, will be informative to further advance our understanding of the role glycogen plays in *Chlamydia* biology (31).

Also of high interest were three transposon insertions in the polymorphic membrane protein ORFs *pmpI*, *pmpA*, and *pmpD*. Pmps comprise a 9-member family of autotransporter adhesins in *C. muridarum* and *C. trachomatis*, and their presence in all sequenced *Chlamydia* strains is suggestive of important functions mediated by each Pmp protein (35, 44). Neutralizing antibodies to Pmps have been shown to be effective at blunting infection (33, 45), and recombinant *C. trachomatis* Pmps were capable of eliciting protective immune responses against *C. muridarum* challenge in mice (46). It has been hypothesized that *pmp* genes may undergo a type of antigenic variation through patterns of transcriptional and/or translational expression (47–50). Our data show that *C. muridarum* lacking *PmpI* exhibited significant growth defects in cell culture. These results are consistent with prior reports that *PmpI* plays a prominent role during *C. trachomatis* infection, particularly under conditions of stress (50). The previous study also showed that the expression of *PmpA*, *PmpD*, and *PmpI* genes was less affected than that of other *pmp* genes in penicillin-stressed cells and suggested that these Pmps might play important functional roles for *Chlamydia* (50). Our data showed that *PmpD* is important for optimal *C. muridarum* growth in culture, whereas *PmpA* was dispensable. The lack of pronounced phenotypes for *pmpD*::Tn substantiates a previous report that a *pmpD*-null strain of *C. trachomatis* had no defect in murine cell culture or in mice (51). The study also reported reduced attachment to human cells and abnormal morphology with the *pmpD*-null mutant, which is somewhat similar to the inclusion morphology obtained in the present study for the *pmpD*::Tn mutant. In summary, our data demonstrate that transposon mutagenesis is a powerful new tool for functional

genetic investigation in *C. muridarum*, in that isogenic mutants can be evaluated for phenotypes in a cell culture system.

MATERIALS AND METHODS

Cell lines and bacterial strains. McCoy cells were cultured in 6-well plates or T-25 flasks in Dulbecco's modified Eagle medium (DMEM) GlutaMax growth medium (Gibco) supplemented with 10% fetal bovine serum (FBS) (full growth medium [FGM]). *C. muridarum* strain Nigg (provided by Kyle Ramsey) was grown in McCoy cells and centrifuged at $700 \times g$ for 30 to 60 min to initiate infection. Following centrifugation, the medium was replaced with fresh FGM supplemented with $1 \mu\text{g/ml}$ cycloheximide.

Transposon mutant generation. *C. muridarum* transposon mutants were generated by transformation of wild-type *C. muridarum* with the transposon vector pCMC5M, using the previously described CaCl_2 transformation system and chloramphenicol for selection (5, 52, 53). Briefly, *C. muridarum* EB ($\sim 2 \times 10^7$ IFU) were mixed with plasmid pCMC ($\sim 10 \mu\text{g}$) in $200 \mu\text{l}$ of CaCl_2 -Tris buffer for 20 to 30 min at room temperature (RT). Meanwhile, approximately 6×10^6 McCoy cells were resuspended in $300 \mu\text{l}$ of CaCl_2 -Tris buffer. The bacterium-plasmid mixture was then added to McCoy cells and incubated at RT for a further 15 min. Finally, the cell-bacterium-plasmid mixture was aliquoted into a 6-well plate with 2 ml FGM in each well. The plate was incubated at 37°C in 5% CO_2 for ~ 2 h before being centrifuged at $700 \times g$ for 30 to 60 min. The plate was placed in the incubator for approximately 6 h, after which the culture medium was replaced with FGM supplemented with $0.5 \mu\text{g/ml}$ chloramphenicol and $1 \mu\text{g/ml}$ cycloheximide. At 30 hpi, cultures from each well were harvested individually for further passages and selections in $0.5 \mu\text{g/ml}$ chloramphenicol. The cultures were frequently and carefully checked for GFP expression on an inverted fluorescence microscope. The isolated mutants were plaque cloned and serially passaged 3 or 4 times through McCoy cells. The resulting clones were expanded and then stored at -80°C until they were used.

Stability test of transposon insertions. Cloned transposon mutants were grown continuously in either the presence or absence of $0.5 \mu\text{g/ml}$ chloramphenicol selection. For each passage, serial dilutions of samples were used to infect McCoy cells in 24-well plates. Samples in the wells with ~ 10 to 20% infection were harvested 24 hpi and then used for the next round of passage. After 10 passages, all the samples were grown in medium without chloramphenicol for genomic-DNA extraction. PCRs were performed using primers flanking the transposon inserts and genomic DNA as templates.

PCR genotyping of mutants. Total genomic DNA was extracted from mutants growing in McCoy cells for sequencing using the primers within the transposon: MCIP_upseq1, 5'-ACACACGGGCACTTTA TAG-3', and Cat_dseq_2, 5'-CAGGGCGGGCGTAAAGATC-3'. The locations of transposon insertions were first predicted by aligning a short sequence right after the transposon inverted repeat (IR) with the sequence of *C. muridarum* Nigg in GenBank (NC_002620) and then confirmed by sequencing using primers on the genome (near the transposon insertions) and PCR using primer sets on the genome flanking the transposon insertions (see Table S2 in the supplemental material).

Whole-genome sequencing. Purified EB were centrifuged at $16,000 \times g$ for 10 min, and the supernatant was discarded. The pellet was resuspended in water and treated with RQ1 DNase (Promega) at 37°C for 30 min. RQ1 stop solution was added to the solution for 10 min at 65°C . Dithiothreitol was added to a final concentration of 5 mM, and the lysates were incubated at 56°C for 1 h. Genomic DNA was then extracted using a DNeasy blood and tissue kit (Qiagen). Whole-genome sequencing templates were prepared using a Nextera XT DNA library preparation (Illumina). Genome sequencing was conducted on an Illumina HiSeq 3000 at the Oregon State University Center for Genome Research and Biocomputing Core. The Illumina-generated reads were filtered and trimmed using Trimmomatic (54). The manicured read files were mapped to the parental strains using the programs Bowtie2 (55) and Trinity (56) and assembled using the bioinformatics software platform Geneious (57). Genome sequences were assembled using a reference-guided approach employing the genome sequence of *C. muridarum* NC_002620 (26).

Generation of complemented strains. Three plasmid vectors, pNigg-mCherry-glgB, pNigg-mCherry-pmpA, and pNigg-mCherry-pmpl, were constructed for complementation studies of three *C. muridarum* transposon mutants in which one of the *glgB*, *pmpA*, and *pmpl* genes was interrupted. The vectors contained a backbone of *C. muridarum* Nigg plasmid CDS2-8, the pUC origin of replication (*ori*), *bla*, and *mCherry*, as well as a genomic gene. These plasmid vectors were transformed into corresponding *C. muridarum* transposon mutants under penicillin selection. The transformants were visualized by red fluorescence from mCherry.

Immunofluorescence and light microscopy. L929 cells were grown to near confluence in an 8-well ibiTreat μ -Slide (Ibidi, Martinsried, Germany) and were infected with the respective wild-type *C. muridarum* or transposon mutant at about 10 to 20 IFU per well. At 24 hpi, the infected cells were fixed with 100% methanol for 10 min at room temperature. The cells were washed once with Hanks balanced salt solution (HBSS) and again with phosphate-buffered saline (PBS) and then stained with PathoDx *Chlamydia* culture confirmation (Remel, Kent, United Kingdom) (Evans blue counterstain and anti-lipopolysaccharide [anti-LPS] GFP-conjugated antibody) diluted 1:40 in PBS overnight at room temperature in the dark. Twenty microliters of $1 \mu\text{M}$ 4',6-diamidino-2-phenylindole (DAPI) diluted 1:100 in PBS was then added to the wells and allowed to stain for 10 min at room temperature in the dark. The stain was then removed, and the cells were washed with PBS. A final overlay of Vectashield antifade mounting medium (Vector, Burlingame, CA) was added, and the slides were immediately imaged. The cells were visualized on an Olympus IX81/31 spinning-disk confocal inverted microscope at $\times 150$ magnification and captured on an Andor (Belfast, Northern Ireland) Zyla 4.2 scientific complementary metal oxide semi-

conductor (sCMOS) camera. The microscope and camera were operated using SlideBook 6 software (Intelligent Imaging Innovations, Denver, CO). Eight to 10 inclusions were imaged for each wild-type *C. muridarum* cell or transposon mutant. The exposure time remained consistent for all fields captured, with exposure for DAPI (DNA) at 1 s, LPS (*Chlamydia*) at 3 s, and cytoplasm (host cell) at 2.5 s. At least 10 z-stack images 0.3 μm apart were taken per imaged field. The images were processed in SlideBook 6 using a no-neighbors deconvolution, with a subtraction constant of 0.4 applied to all the images.

Iodine staining of *Chlamydia*-infected cells. McCoy cells cultured on glass coverslips in individual shell vials were infected with the above-described strains at an MOI of 0.5 and incubated for 26 h. To detect the presence of accumulated glycogen, the medium was removed and the monolayers were rinsed 3 times with PBS and then stained with iodine (58). Briefly, a solution of 50% methanol and 50% iodine was added to the monolayers for 5 min and then removed, and coverslips were mounted with a solution of 50% iodine solution plus 50% glycerol. The iodine-stained cells were immediately imaged using a Nikon digital camera system.

***In vitro* growth profiles of mutants.** The *in vitro* growth profiles of *C. muridarum* transposon insertion mutants were assessed by the IFU propagation ratio, i.e., the number of IFU (inclusions) produced from 1 IFU after infection of McCoy cells for a period of time. All the strains were prepared and grown in parallel to avoid any confounding issues due to host cells, media, or handling. Mutant stocks were grown in parallel in McCoy cells at series dilution in 24-well plates, and the wells with ~10 to 30% infection were chosen for imaging and harvest. At 20 to 22 hpi, 20 GFP images were taken randomly for inclusion counting to estimate the initial IFU in the wells. The samples in the wells were harvested at selected time points (22 h, 24 h, 26 h, and 28 h). To assess the IFU in these time point samples, 6 wells of McCoy cells in a 24-well plate were infected with each sample dilution (1:50, 1:100, 1:200, 1:400, 1:800, and 1:1,600), and the wells with ~10 to 20% infection were chosen for imaging. Again, about 22 hpi, 20 GFP images were taken randomly for inclusion counting. The green inclusions were counted using the Fuji image-processing package (ImageJ).

Cell adherence assays. The attachment efficiencies of the *C. muridarum* mutant strains were measured in the presence or absence of centrifugation, with slight modifications from published procedures (10). McCoy cells were grown in 24-well plates to 90% confluence and washed with HBSS prior to use. *C. muridarum* samples were diluted with a 2-fold dilution series in HBSS, and 0.5 ml of diluted bacteria was inoculated onto McCoy monolayers. A starting MOI of ~1 was used for centrifuged samples and ~100 for static samples. Low-MOI plates were spun at $700 \times g$ for 1 h, after which the cells were incubated with fresh medium containing cycloheximide. High-MOI plates were incubated with *C. muridarum* for 2 h at room temperature without agitation, after which the cells were incubated with fresh medium containing cycloheximide. At 20 to 22 hpi, samples were subjected to live fluorescence microscopy to visualize and image inclusions containing GFP-expressing *C. muridarum*. Ten random images were taken for each sample well at $\times 20$ magnification. Inclusion counts were quantified using ImageJ. From two experiments, five sets of data were calculated from each mutant with similar infection ratios in both centrifuged and noncentrifuged samples.

Statistical analysis. Statistical analysis was performed using GraphPad Prism software. Comparisons between IFU, bacterial attachment, and *in vivo* bacterial burdens were analyzed using one-way analysis of variance (ANOVA) with Dunnett's test for multiple comparisons.

SUPPLEMENTAL MATERIAL

Supplemental material for this article may be found at <https://doi.org/10.1128/JB.00366-19>.

SUPPLEMENTAL FILE 1, PDF file, 0.5 MB.

ACKNOWLEDGMENTS

We thank the Oregon State University Center for Genome Research and Biocomputing for sequencing and bioinformatics assistance.

This work was supported by a grant from the National Institutes of Health, NIAID A1126785, to K. Hybiske and P. S. Hefty.

REFERENCES

- Torrone E, Papp J, Weinstock H, Centers for Disease Control and Prevention. 2014. Prevalence of *Chlamydia trachomatis* genital infection among persons aged 14-39 years—United States, 2007–2012. *MMWR Morb Mortal Wkly Rep* 63:834–838.
- Johnson NB, Hayes LD, Brown K, Hoo EC, Ethier KA, Centers for Disease Control and Prevention. 2014. CDC National Health Report: leading causes of morbidity and mortality and associated behavioral risk and protective factors—United States, 2005–2013. *MMWR Suppl* 63:3–27.
- Bastidas RJ, Valdivia RH. 2016. Emancipating Chlamydia: advances in the genetic manipulation of a recalcitrant intracellular pathogen. *Microbiol Mol Biol Rev* 80:411–427. <https://doi.org/10.1128/MMBR.00071-15>.
- Hoopaw AJ, Fisher DJ. 2015. A coming of age story: Chlamydia in the post-genetic era. *Infect Immun* 84:612–621. <https://doi.org/10.1128/IAI.01186-15>.
- Wang Y, Kahane S, Cutcliffe LT, Skilton RJ, Lambden PR, Clarke IN. 2011. Development of a transformation system for *Chlamydia trachomatis*: restoration of glycogen biosynthesis by acquisition of a plasmid shuttle vector. *PLoS Pathog* 7:e1002258. <https://doi.org/10.1371/journal.ppat.1002258>.
- Wickstrum J, Sammons LR, Restivo KN, Hefty PS. 2013. Conditional gene expression in *Chlamydia trachomatis* using the tet system. *PLoS One* 8:e76743. <https://doi.org/10.1371/journal.pone.0076743>.
- Johnson CM, Fisher DJ. 2013. Site-specific, insertional inactivation of *incA* in *Chlamydia trachomatis* using a group II intron. *PLoS One* 8:e83989. <https://doi.org/10.1371/journal.pone.0083989>.

8. Demars R, Weinfurter J, Guex E, Lin J, Potucek Y. 2007. Lateral gene transfer in vitro in the intracellular pathogen *Chlamydia trachomatis*. *J Bacteriol* 189:991–1003. <https://doi.org/10.1128/JB.00845-06>.
9. DeMars R, Weinfurter J. 2008. Interstrain gene transfer in *Chlamydia trachomatis* in vitro: mechanism and significance. *J Bacteriol* 190:1605–1614. <https://doi.org/10.1128/JB.01592-07>.
10. Jeffrey BM, Suchland RJ, Eriksen SG, Sandoz KM, Rockey DD. 2013. Genomic and phenotypic characterization of in vitro-generated *Chlamydia trachomatis* recombinants. *BMC Microbiol* 13:142. <https://doi.org/10.1186/1471-2180-13-142>.
11. Mueller KE, Wolf K, Fields KA. 2016. Gene deletion by fluorescence-reported allelic exchange mutagenesis in *Chlamydia trachomatis*. *mBio* 7:e01817. <https://doi.org/10.1128/mBio.01817-15>.
12. Kari L, Goheen MM, Randall LB, Taylor LD, Carlson JH, Whitmire WM, Virok D, Rajaram K, Endresz V, McClarty G, Nelson DE, Caldwell HD. 2011. Generation of targeted *Chlamydia trachomatis* null mutants. *Proc Natl Acad Sci U S A* 108:7189–7193. <https://doi.org/10.1073/pnas.1102229108>.
13. Nguyen BD, Valdivia RH. 2012. Virulence determinants in the obligate intracellular pathogen *Chlamydia trachomatis* revealed by forward genetic approaches. *Proc Natl Acad Sci U S A* 109:1263–1268. <https://doi.org/10.1073/pnas.1117884109>.
14. Kokes M, Dunn JD, Granek JA, Nguyen BD, Barker JR, Valdivia RH, Bastidas RJ. 2015. Integrating chemical mutagenesis and whole-genome sequencing as a platform for forward and reverse genetic analysis of *Chlamydia*. *Cell Host Microbe* 17:716–725. <https://doi.org/10.1016/j.chom.2015.03.014>.
15. Abdelrahman YM, Belland RJ. 2005. The chlamydial developmental cycle. *FEMS Microbiol Rev* 29:949–959. <https://doi.org/10.1016/j.femsre.2005.03.002>.
16. Elwell C, Mirrashidi K, Engel J. 2016. *Chlamydia* cell biology and pathogenesis. *Nat Rev Microbiol* 14:385–400. <https://doi.org/10.1038/nrmicro.2016.30>.
17. Stephens RS, Kalman S, Lammel C, Fan J, Marathe R, Aravind L, Mitchell W, Olinger L, Tatusov RL, Zhao Q, Koonin EV, Davis RW. 1998. Genome sequence of an obligate intracellular pathogen of humans: *Chlamydia trachomatis*. *Science* 282:754–759. <https://doi.org/10.1126/science.282.5389.754>.
18. LaBrie SD, Dimond ZE, Harrison KS, Baid S, Wickstrum J, Suchland RJ, Hefty PS. 2019. Transposon mutagenesis in *Chlamydia trachomatis* identifies CT339 as a ComEC homolog important for DNA uptake and lateral gene transfer. *mBio* 10:e01343-19. <https://doi.org/10.1128/mBio.01343-19>.
19. Akerley BJ, Rubin EJ, Camilli A, Lampe DJ, Robertson HM, Mekalanos JJ. 1998. Systematic identification of essential genes by in vitro mariner mutagenesis. *Proc Natl Acad Sci U S A* 95:8927–8932. <https://doi.org/10.1073/pnas.95.15.8927>.
20. Hensel M, Shea JE, Gleeson C, Jones MD, Dalton E, Holden DW. 1995. Simultaneous identification of bacterial virulence genes by negative selection. *Science* 269:400–403. <https://doi.org/10.1126/science.7618105>.
21. Sassetti CM, Boyd DH, Rubin EJ. 2003. Genes required for mycobacterial growth defined by high density mutagenesis. *Mol Microbiol* 48:77–84. <https://doi.org/10.1046/j.1365-2958.2003.03425.x>.
22. Rajaram K, Giebel AM, Toh E, Hu S, Newman JH, Morrison SG, Kari L, Morrison RP, Nelson DE. 2015. Mutational analysis of the *Chlamydia muridarum* plasticity zone. *Infect Immun* 83:2870–2881. <https://doi.org/10.1128/IAI.00106-15>.
23. Conrad TA, Gong S, Yang Z, Matulich P, Keck J, Beltrami N, Chen C, Zhou Z, Dai J, Zhong G. 2016. The chromosome-encoded hypothetical protein TC0668 is an upper genital tract pathogenicity factor of *Chlamydia muridarum*. *Infect Immun* 84:467–479. <https://doi.org/10.1128/IAI.01171-15>.
24. Yang Z, Tang L, Shao L, Zhang Y, Zhang T, Schenken R, Valdivia R, Zhong G. 2016. The *Chlamydia*-secreted protease CPAF promotes chlamydial survival in the mouse lower genital tract. *Infect Immun* 84:2697–2702. <https://doi.org/10.1128/IAI.00280-16>.
25. Shao L, Zhang T, Liu Q, Wang J, Zhong G. 2017. *Chlamydia muridarum* with mutations in chromosomal genes *tc0237* and/or *tc0668* is deficient in colonizing the mouse gastrointestinal tract. *Infect Immun* 85:e00321-17. <https://doi.org/10.1128/IAI.00321-17>.
26. Read TD, Brunham RC, Shen C, Gill SR, Heidelberg JF, White O, Hickey EK, Peterson J, Utterback T, Berry K, Bass S, Linher K, Weidman J, Khouri H, Craven B, Bowman C, Dodson R, Gwinn M, Nelson W, DeBoy R, Kolonay J, McClarty G, Salzberg SL, Eisen J, Fraser CM. 2000. Genome sequences of *Chlamydia trachomatis* MoPn and *Chlamydia pneumoniae* AR39. *Nucleic Acids Res* 28:1397–1406. <https://doi.org/10.1093/nar/28.6.1397>.
27. Nelson DE, Crane DD, Taylor LD, Dorward DW, Goheen MM, Caldwell HD. 2006. Inhibition of chlamydiae by primary alcohols correlates with the strain-specific complement of plasticity zone phospholipase D genes. *Infect Immun* 74:73–80. <https://doi.org/10.1128/IAI.74.1.73-80.2006>.
28. Voigt A, Schöfl G, Saluz HP. 2012. The *Chlamydia psittaci* genome: a comparative analysis of intracellular pathogens. *PLoS One* 7:e35097. <https://doi.org/10.1371/journal.pone.0035097>.
29. Belland RJ, Scidmore MA, Crane DD, Hogan DM, Whitmire W, McClarty G, Caldwell HD. 2001. *Chlamydia trachomatis* cytotoxicity associated with complete and partial cytotoxin genes. *Proc Natl Acad Sci U S A* 98:13984–13989. <https://doi.org/10.1073/pnas.241377698>.
30. Carlson JH, Whitmire WM, Crane DD, Wicke L, Virtaneva K, Sturdevant DE, Kupko JJ, III, Porcella SF, Martinez-Orengo N, Heinzen RA, Kari L, Caldwell HD. 2008. The *Chlamydia trachomatis* plasmid is a transcriptional regulator of chromosomal genes and a virulence factor. *Infect Immun* 76:2273–2283. <https://doi.org/10.1128/IAI.00102-08>.
31. Gehre L, Gorgette O, Perrinet S, Prevost M-C, Ducatez M, Giebel AM, Nelson DE, Ball SG, Subtil A. 2016. Sequestration of host metabolism by an intracellular pathogen. *Elife* 5:e12552. <https://doi.org/10.7554/eLife.12552>.
32. Miyashita N, Matsumoto A, Fukano H, Niki Y, Matsushima T. 2001. The 7.5-kb common plasmid is unrelated to the drug susceptibility of *Chlamydia trachomatis*. *J Infect Chemother* 7:113–116. <https://doi.org/10.1007/s1015610070113>.
33. Mölleken K, Schmidt E, Hegemann JH. 2010. Members of the Pmp protein family of *Chlamydia pneumoniae* mediate adhesion to human cells via short repetitive peptide motifs. *Mol Microbiol* 78:1004–1017. <https://doi.org/10.1111/j.1365-2958.2010.07386.x>.
34. Van Lent S, De Vos WH, Huot Creasy H, Marques PX, Ravel J, Vanrompay D, Bavoil P, Hsia R-C. 2016. Analysis of polymorphic membrane protein expression in cultured cells identifies PmpA and PmpH of *Chlamydia psittaci* as candidate factors in pathogenesis and immunity to infection. *PLoS One* 11:e0162392. <https://doi.org/10.1371/journal.pone.0162392>.
35. Vasilevsky S, Stojanov M, Greub G, Baud D. 2016. Chlamydial polymorphic membrane proteins: regulation, function and potential vaccine candidates. *Virulence* 7:11–22. <https://doi.org/10.1080/21505594.2015.1111509>.
36. Becker E, Hegemann JH. 2014. All subtypes of the Pmp adhesion family are implicated in chlamydial virulence and show species-specific function. *Microbiologyopen* 3:544–556. <https://doi.org/10.1002/mbo3.186>.
37. Hybiske K, Stephens RS. 2007. Mechanisms of host cell exit by the intracellular bacterium *Chlamydia*. *Proc Natl Acad Sci U S A* 104:11430–11435. <https://doi.org/10.1073/pnas.0703218104>.
38. Zuck M, Sherrid A, Suchland R, Ellis T, Hybiske K. 2016. Conservation of extrusion as an exit mechanism for *Chlamydia*. *Pathog Dis* 74:ftw093. <https://doi.org/10.1093/femspd/ftw093>.
39. Luczak SET, Smits SHJ, Decker C, Nagel-Steger L, Schmitt L, Hegemann JH. 2016. The *Chlamydia pneumoniae* adhesion Pmp21 forms oligomers with adhesive properties. *J Biol Chem* 291:22806–22818. <https://doi.org/10.1074/jbc.M116.728915>.
40. Valdivia RH, Bastidas RJ. 2018. The expanding molecular genetics tool kit in *Chlamydia*. *J Bacteriol* 200:e00590-18. <https://doi.org/10.1128/JB.00590-18>.
41. Sturdevant GL, Kari L, Gardner DJ, Olivares-Zavaleta N, Randall LB, Whitmire WM, Carlson JH, Goheen MM, Selleck EM, Martens C, Caldwell HD. 2010. Frameshift mutations in a single novel virulence factor alter the in vivo pathogenicity of *Chlamydia trachomatis* for the female murine genital tract. *Infect Immun* 78:3660–3668. <https://doi.org/10.1128/IAI.00386-10>.
42. Bonner C, Caldwell HD, Carlson JH, Graham MR, Kari L, Sturdevant GL, Tyler S, Zetner A, McClarty G. 2015. *Chlamydia trachomatis* virulence factor CT135 is stable in vivo but highly polymorphic in vitro. *Pathog Dis* 73:ftv043. <https://doi.org/10.1093/femspd/ftv043>.
43. Song L, Carlson JH, Whitmire WM, Kari L, Virtaneva K, Sturdevant DE, Watkins H, Zhou B, Sturdevant GL, Porcella SF, McClarty G, Caldwell HD. 2013. *Chlamydia trachomatis* plasmid-encoded Pgp4 is a transcriptional regulator of virulence-associated genes. *Infect Immun* 81:636–644. <https://doi.org/10.1128/IAI.01305-12>.
44. Grimwood J, Stephens RS. 1999. Computational analysis of the polymorphic membrane protein superfamily of *Chlamydia trachomatis* and *Chla-*

- mydia pneumoniae. *Microb Comp Genomics* 4:187–201. <https://doi.org/10.1089/omi.1.1999.4.187>.
45. Crane DD, Carlson JH, Fischer ER, Bavoil P, Hsia R-C, Tan C, Kuo C-C, Caldwell HD. 2006. Chlamydia trachomatis polymorphic membrane protein D is a species-common pan-neutralizing antigen. *Proc Natl Acad Sci U S A* 103:1894–1899. <https://doi.org/10.1073/pnas.0508983103>.
 46. Pal S, Favaroni A, Tifrea DF, Hanisch PT, Luczak SET, Hegemann JH, de la Maza LM. 2017. Comparison of the nine polymorphic membrane proteins of Chlamydia trachomatis for their ability to induce protective immune responses in mice against a C. muridarum challenge. *Vaccine* 35:2543–2549. <https://doi.org/10.1016/j.vaccine.2017.03.070>.
 47. Vandahl BB, Pedersen AS, Gevaert K, Holm A, Vandekerckhove J, Christiansen G, Birkelund S. 2002. The expression, processing and localization of polymorphic membrane proteins in Chlamydia pneumoniae strain CWL029. *BMC Microbiol* 2:36. <https://doi.org/10.1186/1471-2180-2-36>.
 48. Tan C, Hsia R-C, Shou H, Haggerty CL, Ness RB, Gaydos CA, Dean D, Scurlock AM, Wilson DP, Bavoil PM. 2009. Chlamydia trachomatis-infected patients display variable antibody profiles against the nine-member polymorphic membrane protein family. *Infect Immun* 77:3218–3226. <https://doi.org/10.1128/IAI.01566-08>.
 49. Grimwood J, Olinger L, Stephens RS. 2001. Expression of Chlamydia pneumoniae polymorphic membrane protein family genes. *Infect Immun* 69:2383–2389. <https://doi.org/10.1128/IAI.69.4.2383-2389.2001>.
 50. Carrasco JA, Tan C, Rank RG, Hsia R-C, Bavoil PM. 2011. Altered developmental expression of polymorphic membrane proteins in penicillin-stressed Chlamydia trachomatis. *Cell Microbiol* 13:1014–1025. <https://doi.org/10.1111/j.1462-5822.2011.01598.x>.
 51. Kari L, Southern TR, Downey CJ, Watkins HS, Randall LB, Taylor LD, Sturdevant GL, Whitmire WM, Caldwell HD. 2014. Chlamydia trachomatis polymorphic membrane protein D is a virulence factor involved in early host-cell interactions. *Infect Immun* 82:2756–2762. <https://doi.org/10.1128/IAI.01686-14>.
 52. Xu S, Battaglia L, Bao X, Fan H. 2013. Chloramphenicol acetyltransferase as a selection marker for chlamydial transformation. *BMC Res Notes* 6:377. <https://doi.org/10.1186/1756-0500-6-377>.
 53. Wang Y, Cutcliffe LT, Skilton RJ, Ramsey KH, Thomson NR, Clarke IN. 2014. The genetic basis of plasmid tropism between Chlamydia trachomatis and Chlamydia muridarum. *Pathogens Dis* 72:19–23. <https://doi.org/10.1111/2049-632X.12175>.
 54. Bolger AM, Lohse M, Usadel B. 2014. Trimmomatic: a flexible trimmer for Illumina sequence data. *Bioinformatics* 30:2114–2120. <https://doi.org/10.1093/bioinformatics/btu170>.
 55. Langmead B, Salzberg SL. 2012. Fast gapped-read alignment with Bowtie 2. *Nat Methods* 9:357–359. <https://doi.org/10.1038/nmeth.1923>.
 56. Grabherr MG, Haas BJ, Yassour M, Levin JZ, Thompson DA, Amit I, Adiconis X, Fan L, Raychowdhury R, Zeng Q, Chen Z, Mauceli E, Hacohen N, Gnirke A, Rhind N, di Palma F, Birren BW, Nusbaum C, Lindblad-Toh K, Friedman N, Regev A. 2011. Full-length transcriptome assembly from RNA-Seq data without a reference genome. *Nat Biotechnol* 29:644–652. <https://doi.org/10.1038/nbt.1883>.
 57. Kearse M, Moir R, Wilson A, Stones-Havas S, Cheung M, Sturrock S, Buxton S, Cooper A, Markowitz S, Duran C, Thierer T, Ashton B, Meintjes P, Drummond A. 2012. Geneious Basic: an integrated and extendable desktop software platform for the organization and analysis of sequence data. *Bioinformatics* 28:1647–1649. <https://doi.org/10.1093/bioinformatics/bts199>.
 58. Schachter J, Dawson CR. 1978. Laboratory diagnosis, p 181–220. *In* Schachter J, Dawson CR (ed), *Human chlamydial infections*. PSG Publishing Company, Burlington, MA.